# SHADOW DETECTION AND RADIOMETRIC RESTORATION IN VHR SATELLITE IMAGERY

Tejoram.V[1], E.Venkateswarlu[2], Thara Nair[2], Vinod M Bothale[2]

## Abstract

High spatial resolution satellite imagery provides more information for remote sensing applications, such as object detection, classification, change detection and mapping. The presence of shadow reduces the quantity of data which will be extracted and consequently makes these applications harder or maybe impossible. In this study, a shadow restoration approach for high resolution satellite images is implemented. This approach detects the shadow area and segments the image into regions with respect to the land surface type. Then, shadow restoration is applied for every region considering the degree of correspondence between shadow and neighbouring non-shadow regions. The approach is applied to study areas from CartoSat-2S satellite images. A comparison to the conventional approaches for shadow restoration is performed, and an accuracy assessment is meted out by visual inspection and land-cover classification. The results show that the shadow regions processed using this approach have better appearance and are highly compatible with their surrounding non-shadow regions. In addition, the final accuracy is more than those of the conventional approaches.

Keywords: Shadow Detection, Image Segmentation, Shadow Restoration

Tejoram.V
tejoram1999@gmail.com

E. Venkateswarlu
venkateswarlu_e@nrsc.gov.in

Thara Nair
thara_nair@nrsc.gov.in

Vinod M Bothale
vinod_bothale@nrsc.gov.in

1. Department of Electronics & Communication Engineering, Coimbatore Institute of Technology, Coimbatore 641 014, India

2. Data Processing Area, National Remote Sensing Center (NRSC), ISRO, Hyderabad, India

## Introduction

More often shadows obscure important objects in very high resolution satellite imagery due to sun elevation at the time of acquisition. Also, even if the sun elevation is low, the presence of shadows is unavoidable in urban areas.

The high resolution images being affected by shadows is a main disadvantage in terms of application perspective. Depending on sun elevation and building size, respective building shadow could have significant area being covered in comparison with total image area. Thus shadows' affecting the image becomes critical.

So as to perform a successful change detection using statistic of images or to use one image and extract information from it, it's important to identify shadow areas within the image and restore the radiometry.

## State of the Artwork

The presence of shadow reduces the amount of information that can be extracted and consequently makes these applications more difficult or even impossible [14]. In order to mitigate the presence of shadows while improving the urban target discrimination in multispectral images - First, the image bands are preprocessed in order to highlight their most relevant parts. Second, a shadow detection procedure is performed by using morphological filtering so that a shadow mask is obtained [2]. A new transformation which enables us to detect boundaries of cast shadows in high resolution satellite images is based on color invariant indices. Different radiometric restoration techniques such as Gamma Correction, Linear-Correlation Correction and Histogram Matching are introduced in order to restore the brightness of detected shadow area [6].

Techniques including recursive quadtree image partition, adaptive thresholding, region growing segmentation, mathematical morphology, and local histogram matching are applied to automatically extract the regions of building-cast shadows [9]. Then, large shadow and non-shadow areas in that image are detected and are used for training a supervised classifier (a Support Vector Machine, SVM) that classifies every pixel in the hyperspectral image as shadow or non-shadow. Finally, small holes are filled through image morphological analysis [3].

High-resolution satellite imagery (HRSI) offers great possibilities for urban mapping. Unfortunately, shadows cast by buildings in high-density urban environments obscure much of the information in the image leading to potentially corrupted classification results or blunders in interpretation [5]. Triclass Thresholding technique is used for segmentation and it is based on Otsu's method. Using this iterative method the images are separated into three classes that are foreground region, background region and to-be determined region [1]. Both pixel-based and object-oriented methods were used to evaluate the effects of shadow detection on Quick Bird image classification and spectroradiometric restoration. In each method, shadows were detected, separated and subsequently corrected [12].

## Shadow detection

Cast shadows in optical images result from the light source being blocked by objects and thus, parts of the image are not illuminated by the direct light. These regions are usually among the darkest areas and may be easily misclassified as other dark objects like water. Using a single band of knowledge (panchromatic image) usually doesn't give us enough information to differentiate between shadows and other dark objects, hence multi-band information is used in order to differentiate between shadow regions and other dark areas in multi-band high-resolution satellite images. Using a set of color invariant indices thus using a non-linear transformation to the data and disaggregate the dark regions. To detect the boundaries of shadows within the image, the variance measure is employed as an area statistic for the texture filter. This particular sort of texture filter enables us to spotlight sudden changes between shadow and non-shadow pixels at the boundary of those two regions.

### Color invariant indices

False detections might occur when classification is done using single band information. Therefore, it is desirable to use the data available in several bands of a multi-spectral image to increase the classification's accuracy. Among many color spaces that are invariant to shadow (i.e., convey the spectral or color characteristics of image features, no matter variations in scene illumination condition [4]) like Hue-Saturation-Value (HSV) or ratio of red (R), green (G), and blue (B) bands, it had been determined that the colour space C1,C2,C3 introduced in [7] can be used as the best non-linear transformation for the shadow detection aim. These indices are defined as following:

$$C1 = \arctan\left(\frac{R}{\max(G,B)}\right)$$

$$C2 = \arctan\left(\frac{G}{\max(R,B)}\right)$$

$$C3 = \arctan\left(\frac{B}{\max(R,G)}\right)$$

where R, G, and B correspond to red, green and blue values of each pixel in the image. Fig. 1 shows the color image of an urban area from CartoSat-2S satellite. Fig. 2, 3 and 4 show the same image after the C1, C2, and C3 transformations are applied. These images are used in the next section to identify the shadow boundaries.

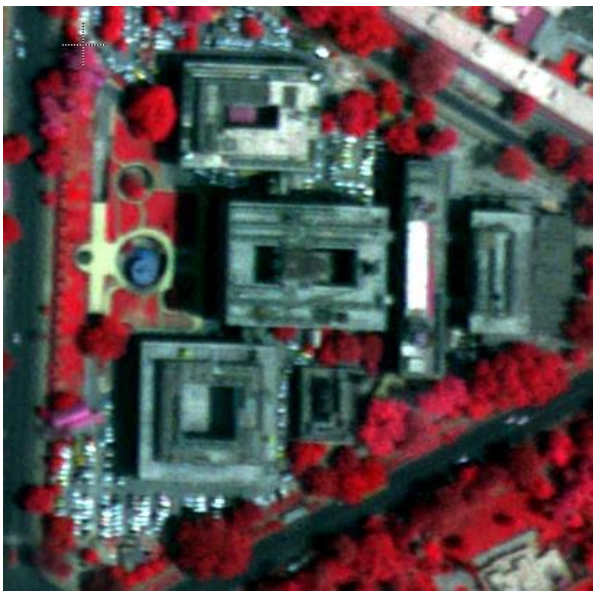

**Fig. 1**: Color image of an urban area

**Fig. 2**: C1Transformation

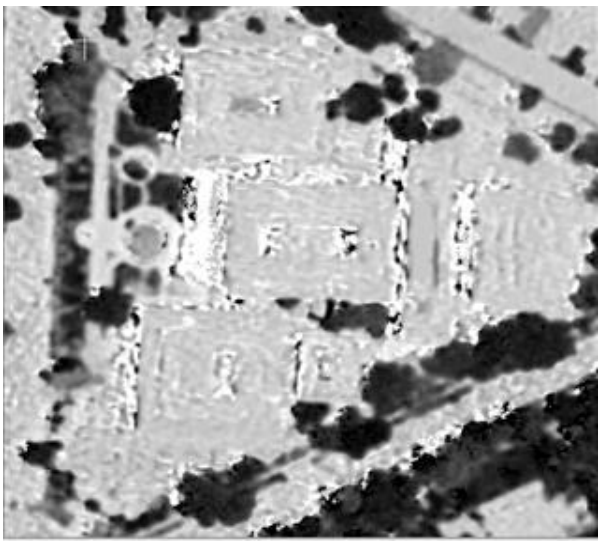

**Fig. 3**: C2 Transformation

**Fig. 4**: C3 Transformation

## Shadow classification

In order to identify shadow boundaries and the region inside those boundaries, the third transformed channel (C3) is used and a 3×3 texture-filter is applied to compute the local variance at the neighborhood of each pixel. The variance filter can be defined as following:

$$\text{Variance} = \frac{1}{N}\sum_{i=0}^{N-1}\sum_{j=0}^{N-1}[f(i,j) - \overline{f(i,j)}]^2$$

where $\overline{f(i,j)} = \frac{1}{N}\sum_{i=0}^{N-1}\sum_{j=0}^{N-1} f(i,j)^2$

A high variance is observed in Digital Number (DN) when there is a huge transition from shadow to non-shadow pixels at the boundary. The resultant is a picture with boundaries of shadow regions as shown in Fig. 5 and 6.

**Fig. 5**: Shadow Boundaries Resulted from applying Generic Filter on the Third Channel (C3)

| | |
|---|---|
| Mean | 0.00729769200272874 |
| Median | 0.0007997616175198772 |
| Range | 0.46611127936668034 |
| Percentile | 0.0002829678616399384 |
| Interquartile Range (IQR) | 0.00292132131981135803 |
| Variance | 0.0005936120407421366 |
| Std. Dev. | 0.024364154833323003 |
| SNR | 0.29952576039078427 |
| Entropy | 17.31214501279328 |
| Min | 0.0 |
| Max | 0.46611127936668034 |

**Table-1**: Statistics of Generic filter result

**Fig. 6**: Shadow Boundaries Resulted from applying Uniform Filter on the Third Channel (C3)

Both generic and uniform filters are applied to the third channel and the results are analyzed statistically. Table-1 and 2 show the statistical information of generic and uniform filters respectively. Because generic filter has non-negative min value, it was chosen on account of programming flexibility.

| | |
|---|---|
| Mean | 0.007297692002729966 |
| Median | 0.000799761617520111 |
| Range | 0.466111279366683 |
| Percentile | 0.00028296786163993346 |
| Interquartile Range (IQR) | 0.00292132131981393 |
| Variance | 0.0005936120407421373 |
| Std. Dev. | 0.024364154833323017 |
| SNR | 0.2995257603907879 |
| Entropy | 17.34432922602658 |
| Min | -2.9976021664879227e-15 |
| Max | 0.46611127936668 |

**Table-2**: Statistics of Uniform filter result

On analyzing histogram of resultant image from both the filters it is very obvious that generic filter produces better results on comparison with uniform filter. Fig. 7 and 8 shows the histogram result of generic and uniform filters respectively.

## Image segmentation

The main aim of the shadow restoration methods is to convert all colors of the shadow image to colors that appear within the non-shadow area. In traditional approaches shadow area is in relation to the non-shadow area with a linear relationship.

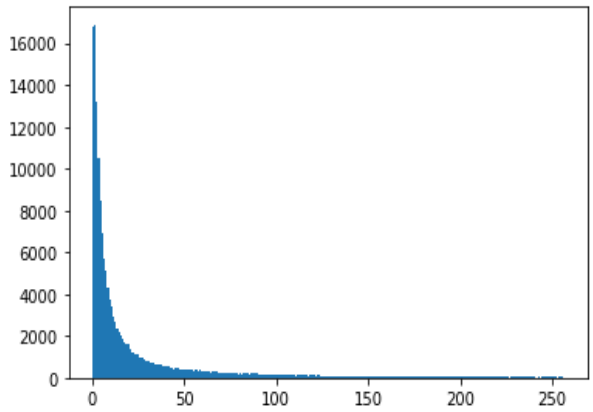


**Fig. 7**: Histogram result of Generic Filter

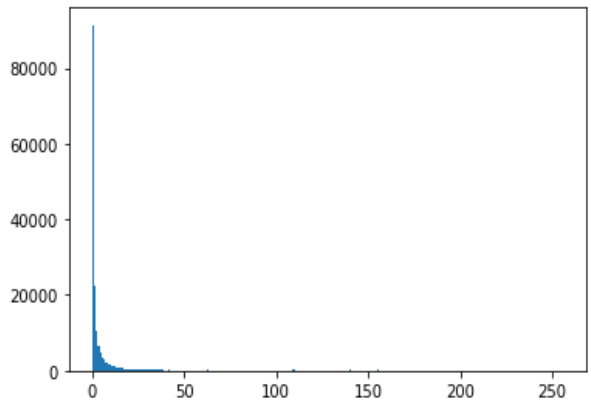


**Fig. 8**: Histogram result of Uniform Filter

In order to calibrate the parameters of this algorithm, lot of pairs of pixel values under sunlight and shadow are extracted from the image. Then, image restoration is applied using the pixel-based method [10]. However, in each class different materials usually have a unique reflectance, which makes global uniform shadow restoration method (without considering the texture and material variation) might not produce satisfactory results. Also, different obstacles existed in one class creates shadows that have different degrees of darkness. As an example, shadow produced by building on a road differs from that produced by trees. Additionally, the darkness of shadow depends heavily on the encircling conditions. Therefore, in complex shadow images, each kind of texture should be handled separately.

This problem is treated by building multiple relationships for every shadow class with the corresponding non-shadow class. For this aim, the region-based method is employed for image restoration rather than using the pixel-based method. The shadowed objects in each class with different brightness are corrected with different ratios to boost the accuracy of the shadow-free image.

Segmentation methods Felzenszwalb's, SLIC, Quickshift and Compact watershed were compared. Restoration results of Compact watershed method outperformed other methods for the dataset. Compact watershed is a region based algorithm. It uses seeds like local gradient minima. Until the seeds reach a border of another seed they grow iteratively pixel by pixel. These borders form the watersheds. Also distance metric is embedded so that they could form equally spaced segments. The distance metric is the weighted combination of the conventional appearance based distance and the euclidean distance of the pixel to the segment seed.

Fig. 9 shows image segmentation by Compact watershed method for various numbers of classes. The higher the numbers of classes better the segmentation. But going for much higher number would separate the object from its corresponding shadow. Thus it brings down the overall restoration accuracy. It is a trade-off between having lower number of classes which causes globalized results vs. higher number of classes which makes restoration impossible or harder. For the example in Fig. 9 class number of 50 is chosen for above reasons.

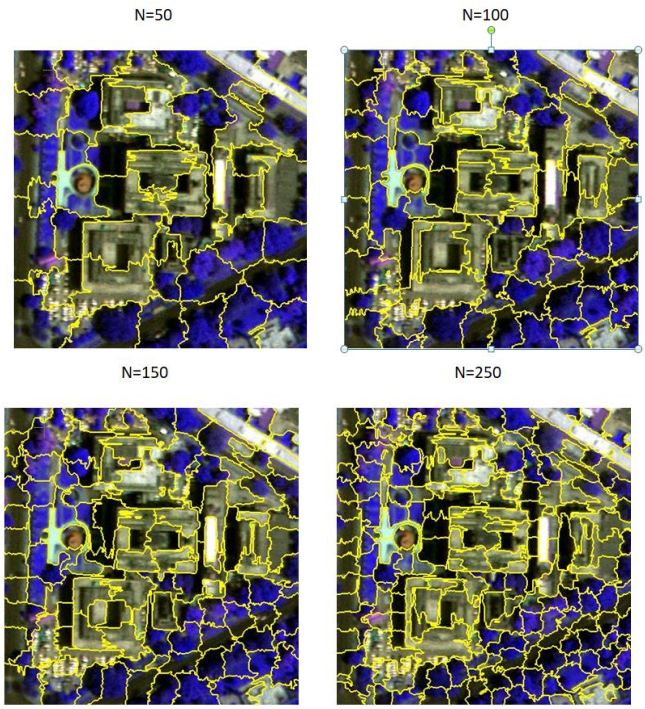


**Fig. 9:** Image segmentation by Compact watershed

## Radiometric Restoration

### Gamma correction

Three different algorithms: Gamma Correction Method, Linear-Correlation Method and Histogram Matching Method are tested in order to radiometrically restore the detected shadow areas. Training data-sets are extracted from the image in order to calibrate the parameters of these algorithms. These parameters should be used for similar regions of the image and may not be applied to the whole image indiscriminately. As example, if parameters are calibrated for the cast shadow of trees on bare-soil, then it should be used only in other areas where trees cast shadows on bare-areas and not on other objects.

The gamma correction persuades the shadow as a multiplicative noise source that corrupts the brightness of the underlying pixels. Therefore, the recovered *DN* values of the shadow regions is given by

$$DNrecovered = (DNshadow)^{\frac{1}{\gamma}}$$

where γ determined from the training data set is the parameter of the algorithm. In practice *DN* values should be normalized, thus, in case of an image with 11-bit dynamic range, the equation can be written as:

$$\frac{DNrecovered}{2047} = \left(\frac{DNshadow}{2047}\right)^{\frac{1}{\gamma}}$$

Only to the class for which parameter γ is computed it should be applied. Using the mean value of shadow pixels and the mean value of neighboring non shadow pixels that are known to represent the shadow pixels, the γ coefficient is estimated.

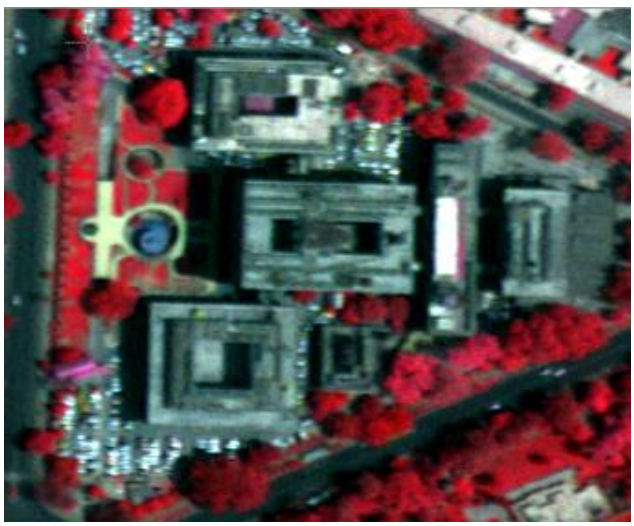

**Fig. 10:** Original Image

**Fig 11:** Gamma Corrected Image

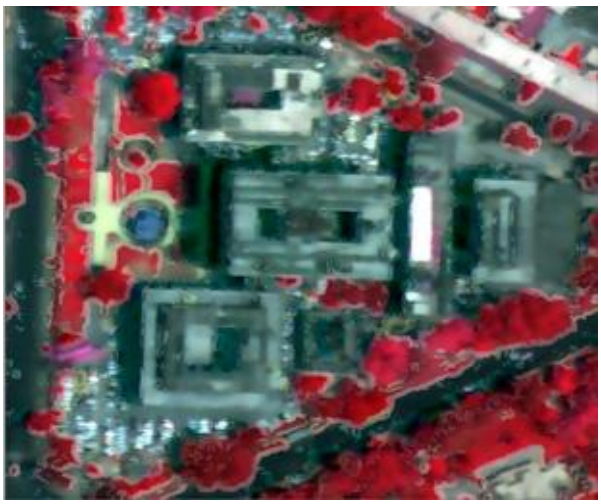

**Fig 12:** Image after applying bilateral filter

**Fig 13:** Image after applying median filter

Shadows on Fig 10 are gamma corrected and the result on Fig 11 is distorted and hence smoothening or blurring filters are applied to remove sharp boundaries and the results are in Fig 12 and Fig 13.

## Linear Correlation correction

If the shadow is modeled as a mixture of additive and multiplicative noise, the brightness of shadow pixels to the first order is restored by a linear function. Using the minimum square error criterion, this linear function can be defined as:

$$DNrecovered = \frac{\sigma nonshadow}{\sigma shadow}(DNshadow - \mu shadow) + \mu nonshadow$$

where μ is the mean value and σ is the standard deviation of the shadow or non-shadow region. The same considerations described previously about case wise application of correction functions should be taken into account.

Shadows on Fig 10 are corrected using linear correlation and the result on Fig 14 is distorted and hence smoothening or blurring filters are applied to remove sharp boundaries and the results are in Fig 15 and Fig 16.

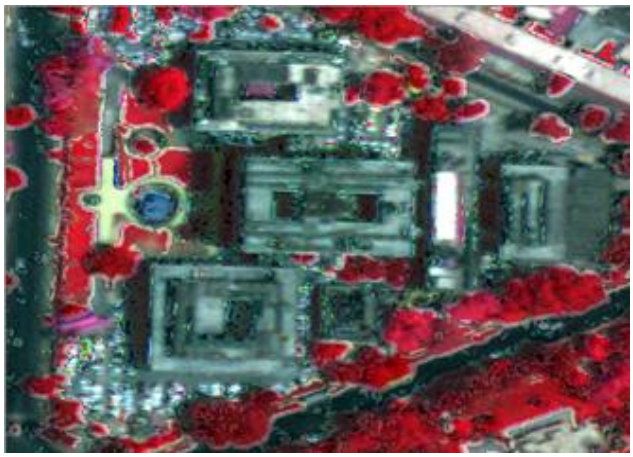

**Fig 14**: Linear Correlation Corrected Image

**Fig 15:** Image after applying bilateral filter

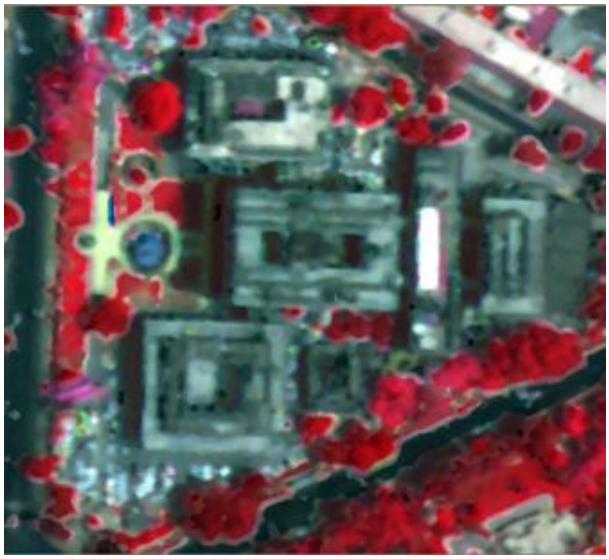

**Fig 16:** Image after applying median filter

## Histogram Matching

Histogram matching is one the classical methods that utilized in order to bring brightness distribution of two given images as close as possible to each other. The proposed method in [8] is employed to recover the DN values of the shadow covered pixels by matching the histogram of the shadow regions to the histogram of the non-shadow areas of the same class. This operation is sensitive to the window size during which the histograms are matched. The Quad-tree partitioning proposed in [9] is applied so as to automatically select the suitable window sizes.

Shadows on Fig 12 are corrected using linear correlation and the result on Fig 17 is distorted and hence smoothening or blurring filters are applied to remove sharp boundaries and the results are in Fig 18 and Fig 19.

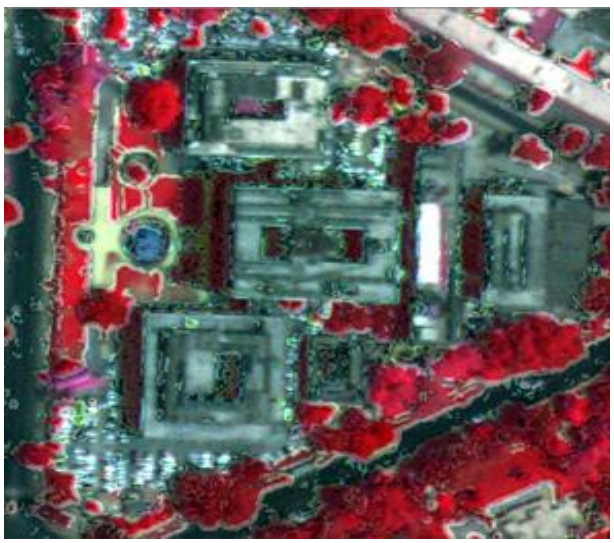

**Fig 17:** Histogram matched image

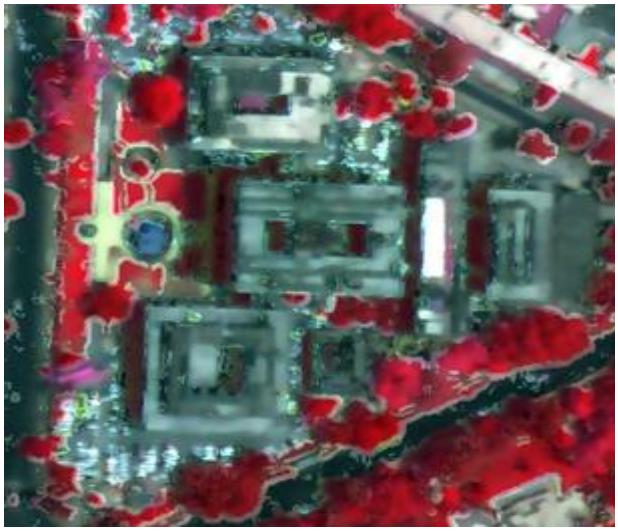

**Fig 18:** Image after applying bilateral filter

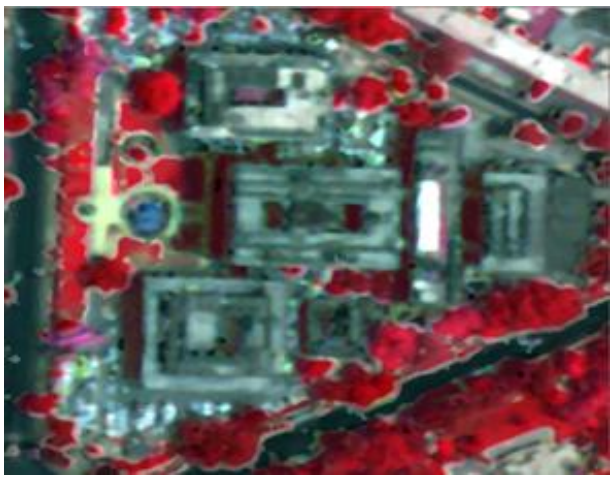

**Fig 19:** Image after applying median filter

Histogram matching occurs on each band of the image separately and the matching process is plotted graphically on Fig 20, 21 and 22.

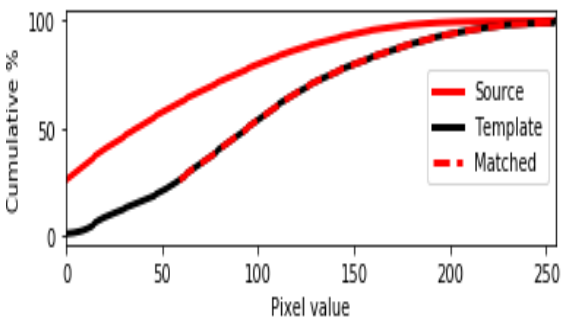


**Fig 20:** Histogram matching of Blue band

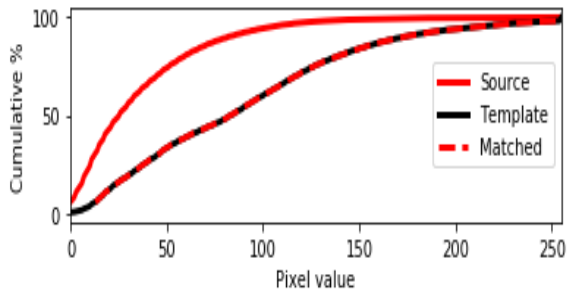


**Fig 21:** Histogram matching of Green band

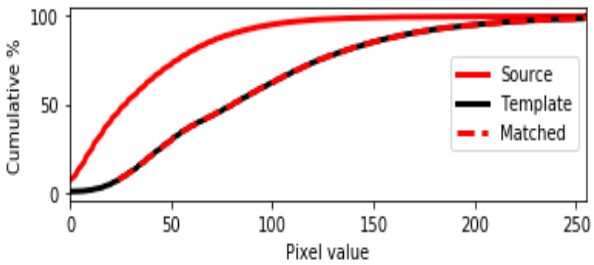


**Fig 22:** Histogram matching of Red band

Where source is the shadow region, template is the non shadow region and matched is the final value of shadow region.

## Data Sets Used

The high-resolution satellite images investigated during this work include CartoSat-2S images with 1.6-meter spatial resolution in multi-spectral bands, 0.6-meter spatial resolution in panchromatic band. The availability of various resolutions and spectra for these images make them particularly suitable candidates for application of the algorithm developed within the study.

## Methodology

The raw data contains both shadow and non shadow part in it. Hence, the shadow and non shadow regions are separated by colour invariant indicies. As local thresholding is desired Image Segmentaion is done to separate individual objects. Then Shadow restoration is done by radiometric restoration methods such as Gamma correction, Linear correlation correction and Histogram matching. Median/Bilateral filter is used to remove sharpness of the image caused by processing. Finally, Quality estimation is done to ensure that the final output is shadow restored and its metrics are not distorted. Then the shadow restored output will be ready for end application.

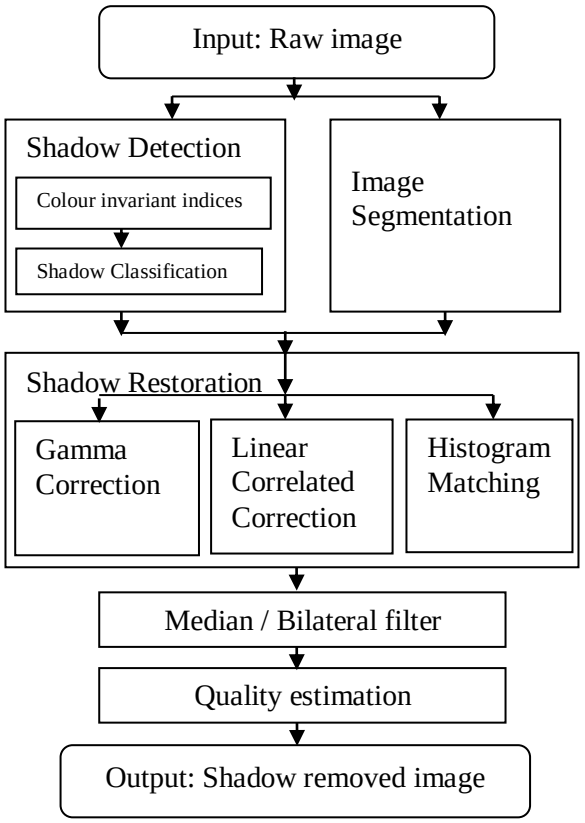


**Fig 23:** Flowchart of Shadow detection and Radiometric Restoration

## Results and Discussion

The study has been carried out in CartoSat-2S with False color composite and Natural color composite images. And observed to be yielding best result at Linear Correlation Corrected Image.

**Fig 24:** Result of False color composite image

Figure 24 is a small portion of Figure 1 taken for analysis and accuracy assessment. In both figure 24 and 25 the top image is original image with shadow, the middle image is shadow detected output and the bottom image is Median/Bilateral filter applied on shadow restored image

**Fig 25:** Result of Natural color composite image

Below Table 3 is the variance and standard deviation of all the four methods that is used while image segmentation.

| **Method** | **Variance** | **Standard Deviation** |
|---|---|---|
| Felzenszwalb's method | 7719.311924821258 | 87.85961486838681 |
| Simple Linear Iterative Clustering | 7201.053375346337 | 84.85902058912968 |
| Quick shift | 9450.829354141122 | 97.21537611993857 |
| Compact Watershed segmentation | 5258.513852422575 | 72.51561109459517 |

**Table-3:**Variance and standard deviation of different segmentation methods

Below table depicts the pixel location in (x,y)- X and Y coordinates and its respective pixel values in the order of (RGB)- Red Green Blue. Sample pixels of shadow and non shadow regions before and after restoration are selected in random manner for analysis. Wherein, it is explicit that shadow pixels after restoration are improved in intensity in comparison with the same shadow pixels before restoration

| **Non-Shadow Pixel info** | **Shadow Pixel location** | **Shadow Pixel info** | **Restored Shadow Pixel info** |
|---|---|---|---|
| 184,41,54 | 27,34 | 3,17,8 | 43,29,29 |
| 107,126,115 | 25,59 | 3,27,14 | 43,58,37 |
| 98,103,76 | 18,17 | 3,0,6 | 43,38,35 |

**Table-4:**Pixel value analysis

Table 5 and 6 represents mean, standard deviation, Signal to Noise Ratio, Entropy and Variance of image before and after shadow restoration respectively. This is done as a part of accuracy assessment with quality metrics.

Fig 26 and 27 are histogram results of image before and after shadow restoration respectively. It is obvious from this histogram comparison to the degree at which shadow restoration is done.

| | |
|---|---|
| Mean | 110.77678831585082 |
| Standard deviation | 74.21614750919773 |
| SNR | 1.4926238026855554 |
| Entropy | 7.820723413026909 |
| Variance | 5508.036551106997 |

**Table-5:**Quality metrics before restoration

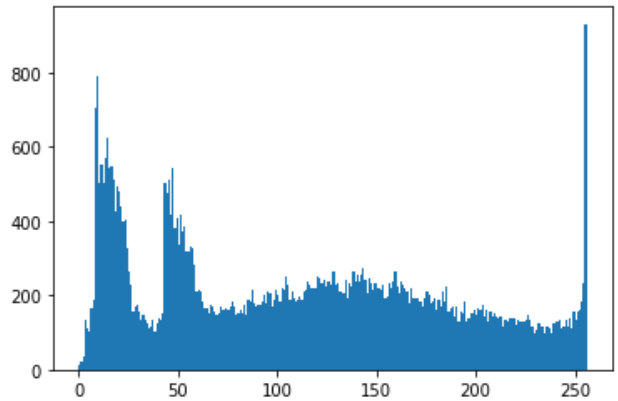


**Fig 26:** Histogram Result of image before resoration

| | |
|---|---|
| Mean | 153.83021925990676 |
| Standard deviation | 42.13187704852461 |
| SNR | 3.6511598826403024 |
| Entropy | 7.393554633408225 |
| Variance | 1775.095063631995 |

**Table-6:**Quality metrics after restoration

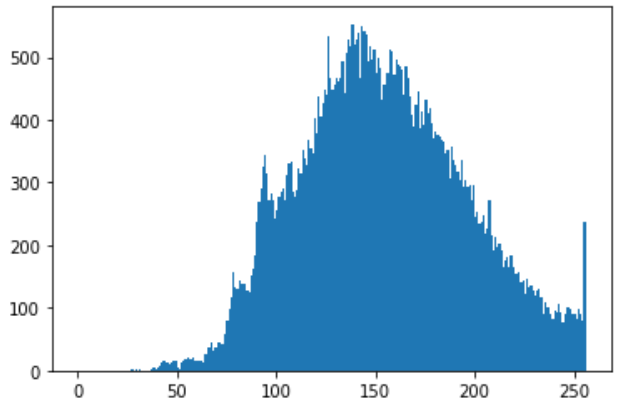


**Fig 27:** Histogram Result of image after restoration

**Table-**7 shows the Kappa, Accuracy and F-measure of the output image this is also used to analyze the quality metrics of the processed output.

| | |
|---|---|
| kappa: | 0.01096398721642744 |
| Accuracy: | 7.968127490039841 |
| F-measure: | 7.889546351084813 |

**Table-7:**Result of Kappa, Accuracy and F-measure

## Conclusion

The change detection problem is one of the applications of shadow restoration. Comparing two high-resolution registered temporal-images for the aim of change detection often can cause false predictions due to the existence of shadows in one image at a given location but not in the second image.

The non-linear transformation C1, C2, C3 provides a color invariant space which is able to discriminate between shadow and other dark objects in the image and is sensitive to shadow. Shadow classification is effective while using the third dimension of this space (C3). By applying texture-filters like variance or edge detector filters the shadow boundaries of the image will be identified. The method uses multi-band rather than single-band information. This approach is an improvement over other methods that use single band information and often misrepresent shadow regions. From the appliance of the shadow restoration methods presented, the most effective results are obtained using the Linear-Correlation Correction method. The Gamma Correlation and Histogram Matching also are able to restore the shadow brightness, but don't seem to be as effective as that of Linear-Correlation method.

## References

[1] Anoopa S, Dhanya V, Dr. Jubilant J Kizhakkethottam. "Shadow Detection and Removal Using Tri-Class Based Thresholding and Shadow Matting Technique." International Conference on Emerging Trends in Engineering, Science and Technology Procedia Technology 24: 1358 – 1365, 2016.

[2] Azevedo, S., Oliveira, R. F., Casaca, W. and Silva, E.T. "Deshadowing of High Spatial Resolution Imagery." Bulletin of Geodetic Sciences, 25(spe): e2019s003, 2019.

[3] Gustav Tolt. "A shadow detection method for remote sensing images using VHR hyperspectral and LIDAR data." Conference: 2011 IEEE International Geoscience and Remote Sensing Symposium, IGARSS 2011, Vancouver, BC, Canada, July 24-29, 2011.

[4] John A. Richards and Xiuping Jia, "Remote Sensing Digital ImageAnalysis", third Ed., Springer-Verlag, Berline, 1999.

[5] Paul M. Dare. "Shadow Analysis in High-Resolution Satellite Imagery of Urban Areas." Photogrammetric Engineering and Remote Sensing, 71(2):169-177, February 2005.

[6] Sarabandi, P., F. Yamazaki, M. Matsuoka, and K. Kiremidjian. "Shadow Detection and Radiometric Restoration in Satellite High Resolution Images." In Proceedings of IEEE International Geoscience and Remote Sensing Symposium (IGARSS '04), Anchorage, AK, USA, 20–24 September 2004; Volume 6: 3744–3747, 2004.

[7] T. Gevers and A. W. M. Smeulders, "Color-based object recognition, pattern recognition", pp. 453–464, 1999.

[8] Thomas M. Lillesand and Ralph W. Kiefer, "Remote Sensing and Image Interpretation", IEEE transaction on Image Processing, Fourth Ed., John Wiley & Sons, 2000.

[9] Victor J.D. Tsai, "Automatic Shadow Detection and RadiometricRestoration on Digital Aerial Images", IGARSS 2003, 2003.

[10] Wan, C. Y., B. A. King, and Z. Li. "An Assessment of Shadow Enhanced Urban Remote SensingImagery of a Complex City— Hong Kong." Proceedings of the XXII Congress of the InternationalSociety for Photogrammetry and Remote Sensing. Melbourne, Australia, 25 August–01 September, pp. 177–182,2012.

[11] Wu, S. T., Y. T. Hsieh, C. T. Ch, and J. C. Chen. "A Comparison of 4 Shadow CompensationTechniques for Land Cover Classification of Shaded Areas from High Radiometric ResolutionAerial Images." Canadian Journal of Remote Sensing 40 (4): 315–326. doi:10.1080/07038992.2014.979488, 2014.

[12] Wu, J., and M. E. Bauer."Evaluating the Effects of Shadow Detection on QuickBird ImageClassification and

Spectroradiometric Restoration."IEEE Journal of Remote Sensing 5: 4450–4469, doi:10.3390/rs5094450, 2013.

[13] Yamazaki, F., W. Liu, and M. Takasaki. "Characteristic of Shadow and Removal of Its Effects forRemote Sensing Imagery."In Proc. International Geoscience and Remote Sensing Symposium, IGARSS, Cape Town, South, Africa, 12–17 July, Vol.9, no. 4, pp. 426–429, 2009.

[14] Yasser Mostafa and Mohamed A. Abdelwahab. "Corresponding regions for shadow restoration in satellite high-resolution images." International Journal of Remote Sensing, 39:20, 7014-7028, DOI: 10.1080/01431161.2018.1471541.

[15] Yuan, F. "Land-Cover Change and Environmental Impact Analysis in the Greater Mankato Area of Minnesota Using Remote Sensing and GIS Modeling." International Journal of Remote Sensing 29 (4): 1169–1184. doi:10.1080/01431160701294703, 2008.